Probing cochlear tuning and tonotopy in the tiger using otoacoustic emissions

Christopher Bergevin
Department of Otolaryngology/Head & Neck Surgery
Columbia University
630 W. 168th St., P&S 11–252
New York, NY 10032
dolemitecb@gmail.com

Edward J. Walsh
JoAnn McGee
Boys Town National Research Hospital
555 North 30th Street
Omaha, NE 68131

Christopher A. Shera
Eaton-Peabody Laboratories
Massachusetts Eye & Ear Infirmary
243 Charles Street
Boston, Massachusetts 02114

Department of Otology & Laryngology
Harvard Medical School
Boston, Massachusetts 02115

Version: May 7, 2012

Abstract

Otoacoustic emissions (sound emitted from the ear) allow cochlear function to be probed noninvasively. The emissions evoked by pure tones, known as stimulus-frequency emissions (SFOAEs), have been shown to provide reliable estimates of peripheral frequency tuning in a variety of mammalian and non-mammalian species. Here, we apply the same methodology to explore peripheral auditory function in the largest member of the cat family, the tiger (*Panthera tigris*). We measured SFOAEs in 9 unique ears of 5 anesthetized tigers. The tigers, housed at the Henry Doorly Zoo (Omaha, Nebraska), were of both sexes and ranged in age from 3–10 yrs. SFOAE phase-gradient delays are significantly longer in tigers—by approximately a factor of two above 2 kHz and even more at lower frequencies—than in domestic cats (*Felis catus*, a species commonly used in auditory studies). Based on correlations between tuning and delay established in other species, our results imply that cochlear tuning in the tiger is significantly sharper than in domestic cat and appears similar to that of humans. Furthermore, the SFOAE data indicate that tigers have a larger tonotopic mapping constant (mm/octave) than domestic cats. A larger mapping constant in tiger is consistent both with auditory brainstem response thresholds (that suggest a lower upper frequency limit of hearing for the tiger than domestic cat) and with measurements of basilar-membrane length (about 1.5 times longer in the tiger than domestic cat).

List of abbreviations

- ABR – auditory brainstem response
- BM – basilar membrane
- DPOAE – distortion-product otoacoustic emission
- ERB – equivalent rectangular bandwidth
- OAE – otoacoustic emission
- SFOAE – stimulus-frequency otoacoustic emission

Introduction

Body mass within the family Felidae varies by more than two orders of magnitude from the smallest to the largest member species. These size differences provide a fertile ground for the comparative and ethological exploration of peripheral auditory function. Studies across a large number of felid species (Huang et al. 1997, 2000, 2002) have shown that middle-ear morphology and hearing performance are related to body size, but much less is known about the variation of inner ear function. As the largest member of the felid family, the tiger is particularly attractive for further investigation. Anatomical studies have provided quantitative estimates of relevant features of the tiger cochlea, such as the length of the basilar membrane (BM) and the number of sensory hair cells (Úlehlová et al. 1984; Walsh et al. 2004). Other experiments have examined auditory evoked potentials (e.g., the auditory brainstem response, or ABR) of tigers and other felids, providing estimates of their frequency ranges of hearing (Walsh et al. 2008, 2011a). Although ABR responses indicate that frequency ranges are broadly similar across felids, tigers have lower high-frequency cut-off frequencies than domestic cats and may have specializations geared towards low-frequency sensitivity (Huang et al. 2000; Walsh et al. 2011a). Such specializations are consistent with the spectral content of tiger vocalizations, which typically contain significant low-frequency (< 1 kHz) energy (Walsh et al. 2011b), a finding consistent with observations from an excised larynx preparation (Titze et al. 2010). Despite these efforts, much is still unknown about auditory physiology in tigers, including cochlear tuning.

The present study exploits the fact that the ear not only responds to sound, but emits sound as well. Sounds emitted by the ear, called otoacoustic emissions (OAEs), can be measured noninvasively in the ear canal using a sensitive, low-noise microphone. Arising either spontaneously or in response to an evoking stimulus, OAEs are generally believed to be a by-product of amplification mechanisms at work in the inner ear (Kemp 1986). Consistent with this notion, healthy ears produce robust emissions, while impaired ears generate little or no sound (Probst et al. 1991). In addition to providing an assay for hearing impairment, OAEs offer a noninvasive means of probing normal cochlear function when direct physiological measurement is otherwise undesirable or impossible. For example, the delays of emissions evoked by pure tones (so-called stimulus-frequency otoacoustic emissions, or SFOAEs) have been shown to predict tuning bandwidths obtained from auditory-nerve recordings in both mammals and non-mammals (Shera et al. 2002, 2010; Bergevin and Shera 2010; Joris et al. 2011).

Our focus here is on tiger SFOAEs. The goal is both to better characterize peripheral auditory function in the tiger and to address several unresolved questions regarding cochlear mechanics and OAE generation. Members of the cat family possess a wide range of basilar-membrane (BM) lengths and, therefore, offer a compelling opportunity to explore whether BM length influences OAEs. Tigers, whose BM extends some 36–39 mm in length (Úlehlová et al. 1984; Walsh et al. 2004)—longer than the nominal values of 35 mm for human and 25 mm for domestic cat—present an especially interesting case to examine how BM length correlates with SFOAE delays and related estimates of cochlear tuning. Because peripheral auditory properties such as the tonotopic map (Liberman 1982) and SFOAEs (Guinan 1990; Shera and Guinan 2003) have been well characterized in domestic cats, comparing responses from domestic cat and tiger provides an opportunity to explore the relationship between cochlear morphology (e.g., BM length) and function (e.g., SFOAE delay, sharpness of tuning).

Methods

Measurements were performed at the Henry Doorly Zoo in Omaha, Nebraska. All procedures were approved by the Institutional Animal Care and Use Committee. Data were collected from 9 ears of 5 tigers (*Panthera tigris*). Three subspecies were examined: the Bengal (*P. tigris tigris*), the Malayan (*P. tigris jacksoni*), and the Amur (*P. tigris altaica*). Two of the animals examined were white-coated tigers having Bengal ancestry. Both male and female individuals were studied, ranging in age from 3–10 years. Animals were immobilized by zoo veterinarians using a blow dart containing a combination of ketamine (24 mg/kg IM), medetomidine (0.05 mg/kg IM), and midazolam (0.1 mg/kg IM). Supplemental doses of ketamine (1 mg/kg IM) were administered as necessary to maintain an immobilized state. Following induction of anesthesia, animals were transported to the Zoo hospital and recording sessions were conducted in an IAC sound-attenuating chamber. After intubation, the inhalation agent sevofluorane mixed with oxygen was used to maintain general anesthesia throughout the measurement session. Recording sessions typically lasted 0.5–2.5 hours. At the completion of each recording session, animals were returned to the holding cage and monitored until fully recovered from anesthesia.

Otoacoustic emissions were measured using Etymōtic ER-10C or ER-10A/ER2 probe systems. A mushroom shaped, flexible probe, roughly 20 mm in diameter, was gently inserted at least 16 mm beyond the

entrance to the external ear canal proper (i.e., the length of the flexible probe). The probe was coated with vaseline to ensure the formation of a closed acoustic coupling. Stimuli were generated and recorded digitally using Lynx L22 sound cards controlled by custom software using a sampling rate of 44.1 kHz. The microphone response was amplified by 40 dB and high-pass filtered with a cutoff frequency of 0.41 kHz to reduce the effects of noise. The probe earphones were calibrated *in-situ* using flat-spectrum, random-phase noise. Calibrations were repeated throughout the measurement session. In control experiments performed in tubes with dimensions and calibration curves similar to the tiger ear canal, we verified that system distortion was at or below the noise floor for the stimulus parameters used here.

Stimulus-frequency OAEs were measured using the suppression paradigm (Shera and Guinan 1999), noting that SFOAE responses are robust to changes in the paradigm used to evoke and extract them (Kalluri and Shera 2007). A probe stimulus level of $L_{\rm p} = 40$ dB SPL was employed, along with the following suppressor parameters: $f_{\rm s} = f_{\rm p} + 40$ Hz and $L_{\rm s} = L_{\rm p} + 15$ dB. This choice of stimulus levels matches previous SFOAE studies in mammals (Shera and Guinan 1999, 2003) that produced acceptable signal-to-noise ratios (SNR); the levels were also low enough to avoid nonlinear effects commonly observed at higher levels (Bergevin et al. 2010). Emissions were measured over the frequency range of 0.7–13 kHz; the lower frequency limit was determined by the acoustic noise floor and the upper limit by the microphone calibration. As a consequence of recording session time limits, we were unable to measure all frequencies in all animals. We sought to optimize the frequency coverage of the total data set by dividing the frequency range into short, 1-kHz segments and measuring them in an irregular order, rather than working systematically from low to high.

At each probe frequency, 35 artifact-free waveforms, each consisting of 8192 samples (approximately 186 ms), were averaged. Waveforms flagged by the artifact-rejection paradigm (Shera and Guinan 1999) were excluded. A settling period of $\sim$20 ms after stimulus onset was inserted before the start of the sampling window to allow the response to reach steady-state. All stimulus frequencies were quantized so that the sample window contained an integral number of stimulus cycles. Frequency step size varied from about 30 Hz at low frequencies to about 60 Hz at high, a resolution fine enough to avoid ambiguity in phase unwrapping. This frequency spacing yielded about 200 data points over the entire frequency range, a resolution equivalent to about 6–7 points per cycle of the emission phase. The noise floor, defined as the average sound-pressure level centered about (but excluding) the frequency of interest, was quantified via averaging

the magnitudes of the adjacent ± 3 bins in the fast Fourier transform of the response.

SFOAE data were collected from a single ear of the first tiger examined (a 3 year old male). However, given the limited access to animals and the short duration of the recording sessions, a dual-recording method was adopted for the subsequent animals. Using this method, OAEs were collected simultaneously from both ears using two separate measurement systems. Data collection for each ear was managed independently by separate investigators; consequently, stimulus presentation across the two ears was unsynchronized. Although the data are limited, SFOAE properties (magnitude, phase, and phase-gradient delay) from the single-ear experiment are comparable to data collected using the dual-ear method in other experiments. This observation, in combination with the relatively low stimulus levels used, suggests that the dual-recording method introduced no significant systematic effects due to efferent activation. This is consistent with previous studies in humans, which show that the effects of contralateral stimulation on ipsilaterally evoked OAEs is small (Guinan et al. 2003; Backus and Guinan 2007; Francis and Guinan 2010).

At the beginning of the measurement session, all animals were screened for the presence of spontaneous OAEs by averaging the spectral magnitudes of 60 artifact-free waveforms, each consisting of 32768 samples (about 743 ms) of data. In the two older tigers, we had time to measure distortion-product OAEs (DPOAEs) using the paradigm described by Bergevin et al. (2008). The primary tones (at frequencies f_1 and f_2, with $f_2/f_1 = 1.22$), and levels $L_1 = L_2 = 65$ dB SPL) were produced by separate earphones using the Etymōtic ER10C probe system. The measurement frequency range, buffer lengths, artifact-rejection and averaging procedures, and noise-floor estimation were all similar to those used for the SFOAE measurements.

Phase-gradient delays were computed via centered-differences (Shera and Guinan 2003). Delays associated with the ear canal length (0.4 ms round trip along the roughly 7 cm long external ear canal, the length measured in one specimen) and the data-acquisition system were subtracted from the total delay.[1] Trends were computed using locally-weighted regression (loess). Confidence intervals (95 %) for the trends were computed using bootstrap resampling to help determine statistical significance when comparing across species. Previous studies have shown that SFOAE delays computed using either a phase-gradient method or measured directly in the time domain match well (Meenderink and Narins 2006; Sisto et al. 2007).

[1]We were unable to measure the lengths of the external ear canals in the tigers studied here. Using a 7-cm estimate obtained from one specimen, and assuming an upper bound of 25% on the tiger-to-tiger variability, yields a corresponding uncertainty of less than 0.1 ms in the round-trip emission delay. At 10 kHz, this corresponds to an uncertainty of about 1 period in N_{SFOAE}, or about 5%. This 5% uncertainty carries over to our estimate of Q_{ERB}.

Results

Typical examples of in-situ earphone calibration curves obtained using the two probe systems are shown in Fig. 1. Figure 2 shows SFOAE magnitudes and phases from individual tigers. SFOAEs were recorded in all animals, each tiger exhibiting a unique and reproducible pattern of magnitude peaks and valleys across frequency. In the three younger animals emission levels were 5–10 dB lower than typically found in humans (Bergevin et al. 2008) and domestic cats (Guinan 1990). In the two older animals (both 10 years old), SFOAE levels were even smaller. We found no age-related effect on SFOAE phase. Although the sample pool is limited, no significant differences in SFOAE properties were apparent with regard to sex, subspecies, or background coat color (i.e., white vs. orange).

When our time with the tigers permitted, we made measurements of several other emission types. Spontaneous OAEs were looked for in all tigers but never observed. Distortion-product emissions (DPOAEs), evoked by two tones and occurring at intermodulation distortion frequencies, were examined in the two older tigers (10 years old) over a limited frequency range (Fig. 3). The magnitudes of the $2f_2 - f_1$ DPOAE were smaller than the $2f_1 - f_2$ but were similar to those of the SFOAEs. At the fixed f_2/f_1 ratio employed, the $2f_1 - f_2$ phase remains almost constant with frequency while $2f_2 - f_1$ exhibits significant phase accumulation. Finally, the tiger $2f_1 - f_2$ distortion product showed no pronounced fine structure, a finding that is consistent with the relatively small magnitude of the SFOAEs observed in the older tigers.

Figure 4 shows the rate of phase accumulation with frequency, also known as the phase-gradient delay. We plot these delays, computed from the slopes of the phase curves shown in Fig. 2, in two different ways: as physical latencies (τ_{SFOAE} in ms) and as the equivalent number of stimulus periods (N_{SFOAE}). [The two are related by the equation $N_{\mathrm{SFOAE}} = f_{\mathrm{p}}\,\tau_{\mathrm{SFOAE}}$, where f_{p} is the probe (emission) frequency.] N_{SFOAE} is a dimensionless quantity useful when comparing delays with the quality factors (Q) commonly used to report tuning bandwidths (e.g., Shera et al. 2002). Although tiger phase-gradient delays $N_{\mathrm{SFOAE}}(f)$ are shorter than those measured in humans (Fig. 5), they are significantly longer than those measured in domestic cats and many other mammals, including chinchillas and guinea pigs (Shera et al. 2010).

Discussion

The goal of the present study was to use OAEs to characterize peripheral auditory function in the tiger. As detailed below, our finding that tiger SFOAE delays are substantially longer than those of domestic cat suggests that tigers have significantly sharper cochlear tuning, and a larger tonotopic mapping constant, than domestic cats. Although tiger SFOAE delays are longer than those of many small mammals, they are shorter than those of humans. Because the tiger basilar membrane is longer than that of humans (Úlehlová et al. 1984; Walsh et al. 2004), BM length alone cannot explain the long delays observed in humans. Since members of the cat family possess a wide range of BM lengths, our results can be extended and tested by measuring SFOAE properties in other felid species (e.g., cats intermediate between domestic cats and tigers, such as lynx and caracal).

Ear canal calibration curves

Earphone calibration curves are included in this report (Fig. 1) because we were surprised not to see evidence of ear-canal standing waves (e.g., deep notches in the measured pressure) due to reflections in the ear canal. As sound propagates down the canal, energy can be reflected off of the canal wall and/or the tympanic membrane and cause standing-wave interference notches at the microphone location due to destructive interference between incident and reflected components. Since the frequencies at which these notches occur depend on the distance between the probe and reflecting surface, the long ear canal of the tiger ($\sim$7 cm) was expected to produce significant standing wave interference in the measured frequency range. Notches created in this way can confound calibrated sound delivery via insert earphones and can lead to erroneous results (Siegel 1994).

Figure 1 shows that although output levels vary with frequency, deep notches are not observed, indicating the absence of standing-wave interference patterns commonly observed in other mammals (Siegel 1994; Ravicz et al. 2007). One possible explanation for the lack of notches is sound attenuation by the canal walls: Energy reflected off the tympanic membrane could be absorbed by the tissue lining the canal on its reverse path back towards the probe. Presumably such attenuation would also affect sound traveling inwards, not an efficient design consideration for an ear canal. Another possibility is that, given the complicated canal geometry and sharp turn [roughly 90°, Huang et al. (2000)], scattering occurs that smooths out peaks and

valleys in the spectral response. Finally, the reflectance at the tympanic membrane may simply be small. The quarter-wave resonance in a 7 cm canal occurs near 1.2 kHz. At frequencies in this range, the single available reflectance measurement in tiger suggests a reflectance magnitude less than 0.05 (Huang et al. 2000).

General emission properties

Since otoacoustic emissions appear to be a universal property of both vertebrate (Koppl 1995; Bergevin et al. 2008) and invertebrate ears (Kössl et al. 2008), their presence in tigers comes as no surprise. Within the present subject pool, the smaller SFOAE magnitudes in the older animals suggests mild hearing loss, perhaps due to noise exposure, or age-related changes in middle ear transmission. Overall, the DPOAE phase properties appear consistent with those obtained from other species (Knight and Kemp 2000; Bergevin et al. 2008).

SFOAE phase-gradient delays

Unlike the N_{SFOAE} values so far reported in other mammalian species, tiger N_{SFOAE} values do not increase smoothly with frequency but manifest a shallow "dip" or plateau near 3–5 kHz. Although our sample size is small enough that the results are subject to statistical fluctuations, the trend line reliably captures the flattening seen in the individual animals. Although the origin of the flattening remains unclear, we hypothesize that it is related to the prominent "notch" seen in measurements of the middle-ear input admittance in tigers and other felids (e.g., Huang et al. 2000). This admittance notch, which occurs just below 3 kHz in the single tiger measured by Huang et al. (2000), is believed to reflect an acoustic resonance between the tympanic cavity and the bulla. In addition to influencing the magnitude of the middle-ear admittance and pressure transfer functions, the resonance produces a rapid phase change that would affect the value of the SFOAE phase-gradient delay at nearby frequencies. Although similar admittance notches occur in domestic cats, which would therefore also be expected to manifest a mid-frequency dip or plateau in their N_{SFOAE} values, the bulla-cavity resonance—along with any effect it may have on SFOAE delay—is eliminated when the bulla is opened widely to the atmosphere, as it was during the measurements of the SFOAE delays in domestic cat shown in Fig. 5.

Estimates of tiger cochlear tuning

Our measurements of tiger SFOAE phase-gradient delays allow us to estimate the sharpness of cochlear tuning. Motivated by principles of filter theory, the procedure takes measurements of N_{SFOAE} and applies the quantitative relationship established in other animals between N_{SFOAE} and the frequency tuning of auditory-nerve fibers (as quantified by values of Q_{ERB}) to infer the values of Q_{ERB} in tiger. The quality factor Q_{ERB} is defined as CF/ERB, where CF is the center or characteristic frequency of a given auditory-nerve fiber and ERB is the fiber's equivalent rectangular bandwidth.[2] More precisely (Shera et al. 2010),

$$Q_{\mathrm{ERB}}(\mathrm{CF}) \approx r_{\mathrm{cat}}(f/\mathrm{CF}_{\mathrm{a|b}})\; N_{\mathrm{SFOAE}}(f)\Big|_{f=\mathrm{CF}} . \tag{1}$$

In this equation, the function r_{cat} is the so-called "tuning ratio" for domestic cat, defined as the ratio $r_{\mathrm{cat}} = Q_{\mathrm{ERB}}/N_{\mathrm{SFOAE}}$ and computed using trend lines fit to cat auditory-nerve and otoacoustic data (Shera and Guinan 2003; Shera et al. 2010). Previous studies have found that the tuning ratio $r(f/\mathrm{CF}_{\mathrm{a|b}})$ has nearly the same form in all mammals studied to date, including cats, guinea pigs, chinchillas, macaques, and humans (Shera et al. 2010; Joris et al. 2011). We assume here that the tiger is no exception. The constant $\mathrm{CF}_{\mathrm{a|b}}$ is a species dependent parameter that divides the cochlea into regions of apical-like and basal-like behavior (Shera et al. 2010). In other species, the approximate value of $\mathrm{CF}_{\mathrm{a|b}}$ can be estimated from the location of a "bend" in the function N_{SFOAE}. In tiger, however, the presence of the mid-frequency "plateau" in N_{SFOAE}—the plateau hypothesized to originate in a middle-ear cavity resonance—makes estimation of $\mathrm{CF}_{\mathrm{a|b}}$ difficult. We therefore compute results for two different values that span the likely range.

The estimates of tiger Q_{ERB} obtained from Eq. (1) are given in Fig. 6 (black lines). As might be anticipated from the tiger's longer OAE delays, our analysis predicts that cochlear tuning in tigers is significantly sharper than in domestic cats and approaches that in humans. Although these qualitative conclusions about cochlear tuning in the tiger appear robust, some quantitative details remain uncertain. For example, the figure shows that the predicted values of Q_{ERB} depend somewhat on the parameter $\mathrm{CF}_{\mathrm{a|b}}$. The solid line assumes that $\mathrm{CF}_{\mathrm{a|b}}$ in tiger is similar to that in domestic cat (i.e., about 3 kHz); the dotted line uses a smaller value similar to that in humans (i.e., near 1–1.5 kHz). In addition, the mid-frequency plateau or dip in the es-

[2]The ERB is a parameter-free measure of tuning bandwidth commonly adopted in the psychophysical literature. For any filter, the ERB is the bandwidth of the rectangular filter with the same peak response that passes the same total power when driven by white noise (Shera et al. 2010).

timated values of Q_{ERB}, especially evident when using $\mathrm{CF_{a|b}} = 3$ kHz, carries over from the similar plateau seen in tiger N_{SFOAE} values. If the plateau in N_{SFOAE} results from a middle-ear cavity resonance, or from some other cause unrelated to cochlear tuning, as we hypothesize, then the predicted plateau in Q_{ERB} is entirely spurious, and no such feature would occur in measurements of tiger Q_{ERB} actually obtained from the auditory nerve. Sharp tuning could have important consequences for a tiger's ability to discern features of complex stimuli, especially in noisy or reverberant environments.

Slope of the tiger cochear map

Returning to the theme of "size" sounded at the outset, we suggest that the relative sharpness of tuning in tiger and domestic cat is related to the parameters of their cochlear tonotopic maps. In many mammals, the sharpness of cochlear tuning correlates with the slope (in mm/octave)[3] of the cochlear map (Shera et al. 2010). The reason may simply be one of real estate. A cochlea with a larger mapping constant (i.e., from a species with a longer cochlea and/or a smaller frequency range of audition) devotes more space to each octave. Since the distance between sensory hair cells ($\approx$10 μm) varies relatively little across mammals, more millimeters per octave means more hair cells per octave—or, to put it inversely, fewer octaves per hair cell. Thus, the hair cells in a cochlea with a larger mapping constant might be expected to have sharper tuning. Unless the tiger is an outlier, our results therefore predict that the mapping constant, or slope, of the tiger cochlear map is greater than that of domestic cat. This conclusion is consistent both with the anatomical observation that tigers have a longer BM than domestic cats (Úlehlová et al. 1984; Walsh et al. 2004) and with ABR data, which indicate that the upper frequency limit of hearing in tiger is somewhat lower than that of domestic cat (Walsh et al. 2008, 2011a).

[3]Several studies examining the mammalian tonotopic map have suggested that it can deviate from a simple exponential form at frequencies below about a few hundred Hz (Greenwood 1990), potentially facilitating sensitivity and selectivity across frequency (Lepage 2003; Vater and Kössl 2011). However, deviations from an exponential map appear not to occur in several small mammals such as guinea pig (Tsuji and Liberman 1997), mouse (Müller et al. 2005), and chinchilla (Müller et al. 2010). It is not known whether significant deviations from an exponential map are present in the tiger cochlea, or if tigers can be considered 'auditory specialists' (Vater and Kössl 2011) for other reasons (Walsh et al. 2011a). While a transition in cochlear processing between the base and apex (e.g., loss of scaling invariance) occurs in the mammalian cochlea (Shera and Guinan 2003; Temchin et al. 2008; Shera et al. 2010), the existence of the transition has not been shown to correlate with deviations from an exponential tonotopic map.

Acknowledgements

The support, advice, and assistance of the veterinarians and staff of the Henry Doorly Zoo were invaluable to the completion of this study. All procedures were approved by the Institutional Animal Care and Use Committee. We thank Sebastiaan Meenderink and John Rosowski for helpful comments on the manuscript. The work was supported by the National Science Foundation (grants 0823417 and 0602173), the Howard Hughes Medical Institute (grant 52003749), and the National Institutes of Health (grants R01 DC003687 and P30 DC05209).

References

Backus BC, Guinan JJ (2007) Measurement of the distribution of medial olivocochlear acoustic reflex strengths across normal-hearing individuals via otoacoustic emissions. J Assoc Res Otolaryngol 8:484–496

Bergevin C (2011) Comparison of otoacoustic emissions within gecko subfamilies: Morphological implications for auditory function in lizards. J Assoc Res Otolaryngol 12:203–217

Bergevin C, Freeman DM, Saunders JC, Shera CA (2008) Otoacoustic emissions in humans, birds, lizards, and frogs: Evidence for multiple generation mechanisms. J Comp Physiol A 194:665–683.

Bergevin C, Shera CA (2010) Coherent reflection without traveling waves: On the origin of long-latency otoacoustic emissions in lizards. J Acoust Soc Am 127, 2398–2409

Bergevin C, Velenovsky D, Bonine KE (2010) Tectorial membrane morphological variation: Effects upon stimulus frequency otoacoustic emissions. Biophys J 99(4):1064–1072

van Dijk P, Mason MJ, Schoffelen RL, Narins PM, Meenderink SWF (2011) Mechanics of the frog ear. Hear Res 273:46–58

Francis NA, Guinan JJ (2010) Acoustic stimulation of human medial olivocochlear efferents reduces stimulus-frequency and click-evoked otoacoustic emission delays: Implications for cochlear filter bandwidths. Hear Res 267:36–45

Greenwood DD (1990) A cochlear frequency-position function for several species—29 years later. J Acoust Soc Am 87:2592–2605

Guinan JJ (1990) Changes in stimulus frequency otoacoustic emissions produced by two-tone suppression and efferent stimulation in cats. In: Dallos P, Geisler CD, Matthews JW, Ruggero MA, Steele CR (eds), Mechanics and Biophysics of Hearing, New York: Springer–Verlag, 170–177

Guinan JJ, Backus B, Lilaonitkul W, Aharonson V (2003) Medial olivocochlear efferent reflex in humans: Otoacoustic emission (OAE) measurement issues and the advantages of stimulus frequency OAEs. J Assoc Res Otolaryngol 4:521–540

Huang GT, Rosowski JJ, Flandermeyer DT, Lynch TJ, Peake WT (1997). The middle ear of a lion: Comparison of structure and function to domestic cat. J Acoust Soc Am 101:1532-1549

Huang GT, Rosowski JJ, Peake WT (2000) Relating middle-ear acoustic performance to body size in the cat family: Measurements and models. J Comp Physiol A 186:447–465

Huang GT, Rosowski JJ, Ravicz ME, Peake WT (2002) Mammalian ear specializations in arid habitats: Structural and functional evidence from sand cat *Felis margarita*, J Comp Physiol A 188:663–681

Joris PX, Bergevin C, Kalluri R, McLaughlin M, Michelet P, van der Heijden M, Shera CA (2011) Frequency selectivity in Old-World monkeys corroborates sharp cochlear tuning in humans. Proc Nat Acad Sci USA 108:17516–17520

Kalluri R, Shera CA (2007) Comparing stimulus-frequency otoacoustic emissions measured by compression, suppression, and spectral smoothing. J Acoust Soc Am 122:3562–3575

Kemp DT (1986) Otoacoustic emissions, travelling waves and cochlear mechanisms. Hear Res 22:95–104

Knight RD, Kemp DT (2000) Indications of different distortion product otoacoustic emission mechanisms from a detailed f_1, f_2 area study. J Acoust Soc Am 107:457–473

Köppl C (1995) Otoacoustic emissions as an indicator for active cochlear mechanics: A primitive property of vertebrate auditory organs, In: Manley GA, Klump GM, Köppl K, Fastl H, Oeckinghaus H (eds), Advances in Hearing Research, Singapore: World Scientific, 207–218

Kössl M, Moeckel D, Weber M, Seyfarth EA (2008) Otoacoustic emissions from insect ears: Evidence of active hearing? J Comp Physiol A 194:597–609

Lepage EL (2003) The mammalian cochlear map is optimally warped. J Acoust Soc Am 114:896–906

Liberman MC (1982) The cochlear frequency map for the cat: Labeling auditory-nerve fibers of known characteristic frequency. J Acoust Soc Am 72:1441–1449

McBrearty AR, Penderis J (2011) Evaluation of auditory function in a population of clinically healthy cats using evoked otoacoustic emissions. J Feline Med Surg 13:919–926

Meenderink SW, Narins PM (2006) Stimulus frequency otoacoustic emissions in the Northern leopard frog, *Rana pipiens pipiens*: Implications for inner ear mechanics. Hear Res 220:67–75

Müller M, Hoidis S, Smolders JW (2010) A physiological frequency-position map of the chinchilla cochlea. Hear Res 268:184–193

Müller M, von Hünerbein K, Hoidis S, Smolders JW (2005) A physiological place-frequency map of the cochlea in the CBA/J mouse. Hear Res 202:63–73

Probst R, Lonsbury-Martin, BL, Martin, GK (1991) A review of otoacoustic emissions. J Acoust Soc Am 89:2027–2067

Ravicz ME, Olson ES, Rosowski JJ (2007) Sound pressure distribution and power flow within the gerbil ear canal from 100 Hz to 80 kHz. J Acoust Soc Am 122:2154–2173

Ruggero MA and Temchin AN (2005) Unexceptional sharpness of frequency tuning in the human cochlea. Proc Nat Acad Sci USA 102:18614–18619

Ruggero MA, Temchin AN (2007) Similarity of traveling-wave delays in the hearing organs of humans and other tetrapods. J Assoc Res Otolaryngol 8:153–166

Shera CA, Guinan JJ (1999) Evoked otoacoustic emissions arise by two fundamentally different mechanisms: A taxonomy for mammalian OAEs. J Acoust Soc Am 105:782–798

Shera CA, Guinan JJ (2003) Stimulus-frequency-emission group delay: A test of coherent reflection filtering and a window on cochlear tuning. J Acoust Soc Am 113:2762–2772

Shera CA, Guinan JJ, Oxenham AJ (2002) Revised estimates of human cochlear tuning from otoacoustic and behavioral measurements. Proc Nat Acad Sci USA 99:3318–3323

Shera CA, Guinan JJ, Oxenham AJ (2010) Otoacoustic estimation of cochlear tuning: Validation in the chinchilla. J Assoc Res Otolaryngol 11:343–365

Siegel JH (1994) Ear-canal standing waves and high-frequency sound calibration using otoacoustic emission probes. J Acoust Soc Am 95:2589–2597

Sisto R, Moleti A, Shera CA (2007) Cochlear reflectivity in transmission-line models and otoacoustic emission characteristic time delays. J Acoust Soc Am 122:3554–3561

Temchin AN, Rich NC, Ruggero MA (2008) Threshold tuning curves of chinchilla auditory-nerve fibers. I. Dependence on characteristic frequency and relation to the magnitudes of cochlear vibrations. J Neurophysiol 100:2889–2898

Titze IR, Fitch WT, Hunter EJ, Alipour F, Montequin D, Armstrong DL, McGee J, Walsh EJ (2010) Vocal power and pressure-flow relationships in excised tiger larynges. J Exp Biol 213:3866–3873

Tsuji J, Liberman MC (1997) Intracellular labeling of auditory nerve fibers in guinea pig: Central and peripheral projections. J Comp Neurol 381:188–202

Úlehlová L, Burda H, Voldich L (1984) Involution of the auditory neuro-epithelium in a tiger (Panthera tigris) and a jaguar (Panthera onca). J Comp Pathol 94:153–157

Vater M, Kössl M (2011) Comparative aspects of cochlear functional organization in mammals. Hear Res 273:89–99

Walsh EJ, Armstrong DL, Napier J, Simmons LG, Korte M, McGee J (2008) Acoustic communication in *Panthera tigris*: A study of tiger vocalization and auditory receptivity revisited. J Acoust Soc Am 123:3507

Walsh EJ, Ketten DR, Arruda J, Armstrong DL, Curro T, Simmons, LG, Wang LM, McGee J (2004) Temporal bone anatomy in *Panthera tigris*. J Acoust Soc Am 115:2485–2486

Walsh EJ, Armstrong DL, McGee J (2011a) Comparative cat studies: Are tigers auditory specialists? J Acoust Soc Am 129:2447

Walsh EJ, Armstrong DL, McGee J (2011b) Tiger bioacoustics: An overview of vocalization acoustics and hearing in *Panthera tigris*. 3rd Symposium on Acoustic Communication by Animals , Cornell University, Ithaca, NY, 173-174

West CD (1985) The relationship of the spiral turns of the cochlea and the length of the basilar membrane to the range of audible frequencies in ground dwelling mammals. J Acoust Soc Am 77:1091–1101

Figure Captions

1. Earphone calibration curves obtained in-situ from two different tigers using two different OAE probe assemblies. The ordinate indicates output for a 1 V rms drive. Dark curves are for an Etymōtic ER-10C, while the grey curves are from an assembly housing an Etymōtic ER-10A microphone and two Etymōtic ER2 earphones.

2. Tiger SFOAEs (magnitude and phase) measured at $L_{\mathrm{p}} = 40$ dB SPL. Data are from 9 ears from 5 tigers. The dashed curve shows an estimate of the mean noise floor obtained by loess smoothing the noise floors measured in the individual animals. Data from the three younger tigers (one 3 year old, two 5 year olds) are indicated by darker shading and the data from the older tigers (two 10 year old tigers) by lighter shading. Individual phase curves were shifted vertically by an integer number of cycles to maximize their overlap.

3. Tiger DPOAEs from the two older animals. The figure shows the magnitude and phase of both the lower- and upper-side band cubic distortion products ($2f_1 - f_2$, dark curves; $2f_2 - f_1$, grey curves). The dashed line provides an estimate of the mean noise floor obtained by loess smoothing. The phase curves have been corrected for approximate ear-canal delays. The stimulus parameters were $L_1 = L_2 = 65$ dB SPL and $f_2/f_1 = 1.22$.

4. Tiger SFOAE phase-gradient delays computed from the phases shown in Fig. 2, expressed either in milliseconds (A) or stimulus periods (B). Only points whose corresponding magnitude was at least 10 dB above the noise floor are included. Thick lines indicate loess trends, thin lines 95% confidence intervals computed via bootstrap resampling.

5. Tiger SFOAE phase-gradient delays (N_{SFOAE}, in periods) compared to those in humans and domestic cats. in stimulus periods (N_{SFOAE}). Data points and loess trends are shown for each species. The data for human and domestic cat are from Shera and Guinan (2003) and were measured using the same paradigms and stimulus levels (40 dB SPL) used here for tiger. Although the confidence intervals for the trends are excluded for clarity, there is no overlap between them for any of the three species at any of the frequencies tested.

6. Otoacoustic estimates of Q_{ERB} for tiger. Estimated values of Q_{ERB} were computed from the measured values of N_{SFOAE} using Eq. (1) and the assumption that tiger tuning ratios are the same as those of domestic cat. Results are shown for two different values of the apical-basal transition CF: The solid black line assumes $\mathrm{CF}_{\mathrm{a|b}} = 3\,\mathrm{kHz}$, similar to domestic cat; the dotted black line assumes $\mathrm{CF}_{\mathrm{a|b}} = 1\,\mathrm{kHz}$, similar to human. Q_{ERB} trends for cat and human are shown for comparison. The cat Q_{ERB} trend was obtained from auditory-nerve fiber (ANF) data (Shera and Guinan 2003; Joris et al. 2011); the human values derive from otoacoustic estimates and behavioral experiments (Shera et al. 2002, 2010).

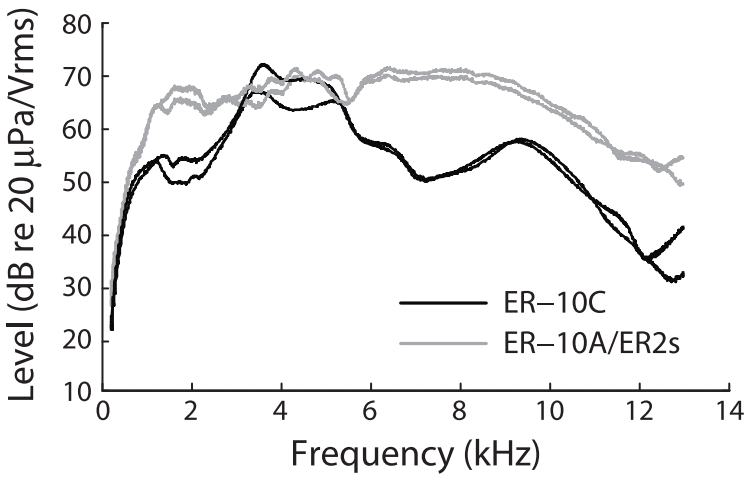
Level (dB re 20 µPa/Vrms)
80
70
60
50
40
30
20
10
0
2
4
6
8
10
12
14
Frequency (kHz)
ER–10C
ER–10A/ER2s

Figure 1

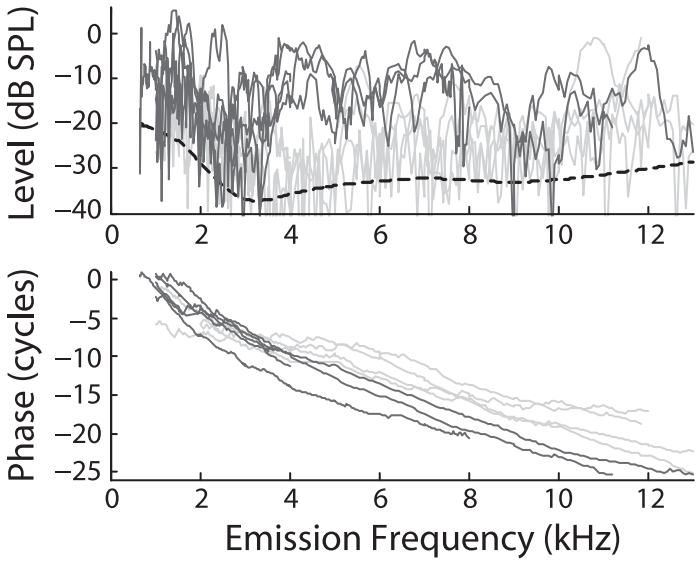
Level (dB SPL)
0
−10
−20
−30
−40
0
2
4
6
8
10
12
Phase (cycles)
0
−5
−10
−15
−20
−25
0
2
4
6
8
10
12
Emission Frequency (kHz)

Figure 2

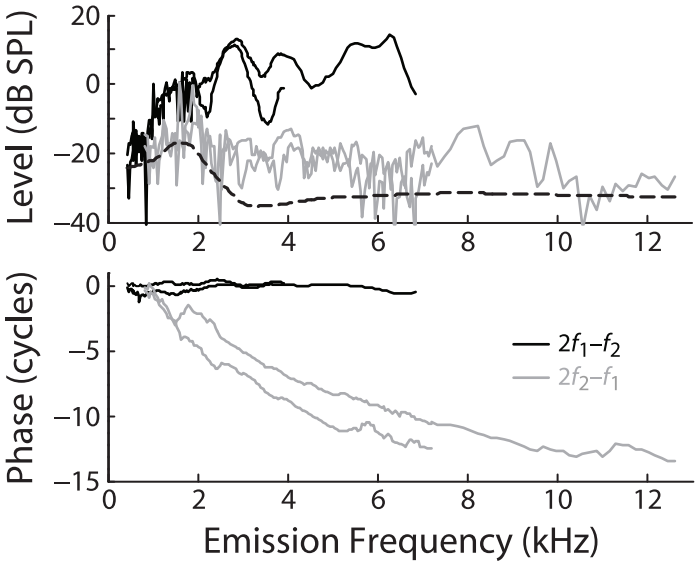
Level (dB SPL)
20
0
−20
−40
0
2
4
6
8
10
12
Phase (cycles)
0
−5
−10
−15
$2f_1-f_2$
$2f_2-f_1$
Emission Frequency (kHz)

Figure 3

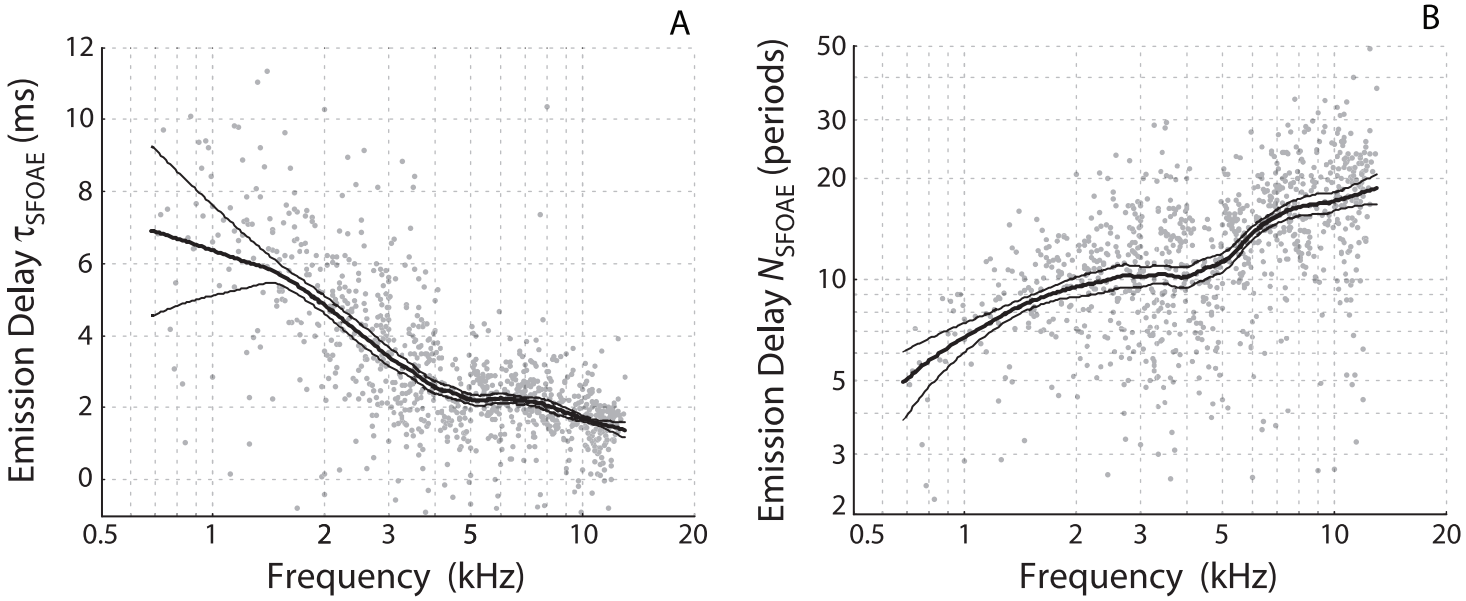
A
B
Emission Delay τ_{SFOAE} (ms)
Emission Delay N_{SFOAE} (periods)
Frequency (kHz)
Frequency (kHz)
0.5
1
2
3
5
10
20
0
2
4
6
8
10
12
2
3
5
10
20
30
50

Figure 4

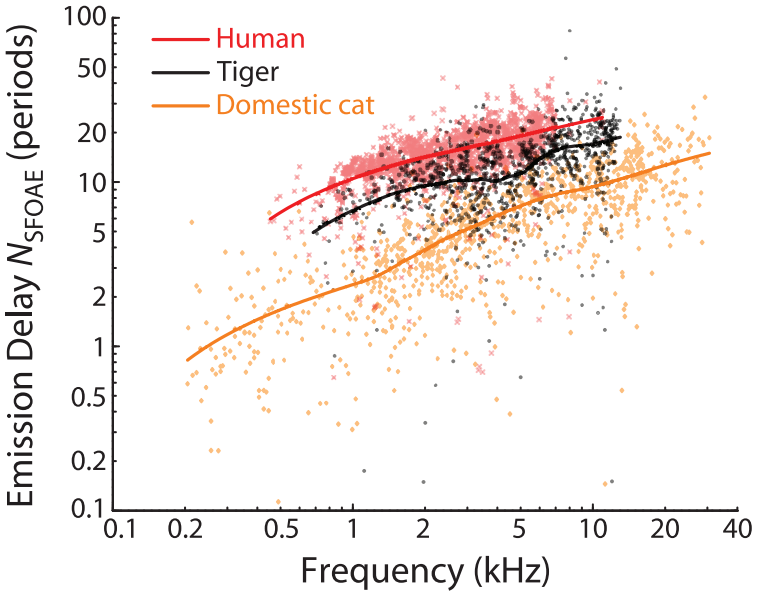
Human
Tiger
Domestic cat
Emission Delay N_{SFOAE} (periods)
100
50
20
10
5
2
1
0.5
0.2
0.1
0.1
0.2
0.5
1
2
5
10
20
40
Frequency (kHz)

Figure 5

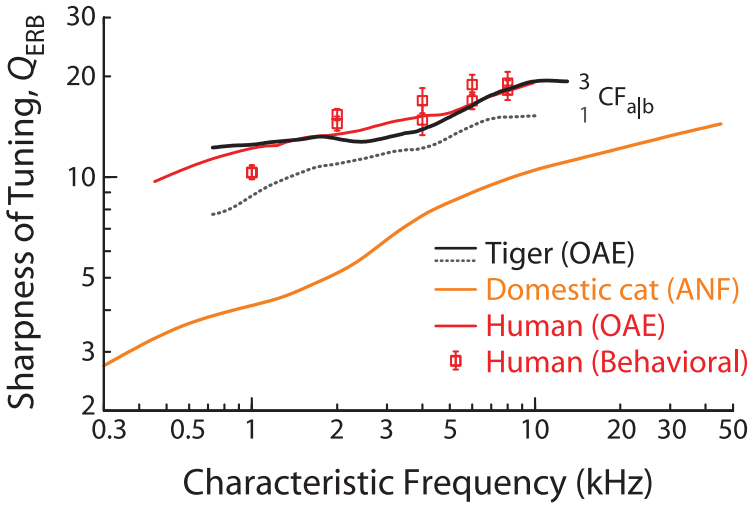
Sharpness of Tuning, Q_{ERB}
30
20
10
5
3
2
0.3
0.5
1
2
3
5
10
20
30
50
Characteristic Frequency (kHz)
3
1
CF$_{a|b}$
Tiger (OAE)
Domestic cat (ANF)
Human (OAE)
Human (Behavioral)

Figure 6